ICANS-XIII
13th Meeting of the International Collaboration on
Advanced Neutron Sources
October 11-14, 1995
Paul Scherrer Institute, 5232 Villigen PSI, Switzerland

Measurements of Spallation Neutrons from a Thick Lead Target Bombarded with 0.5 and 1.5 GeV Protons

Shin-ichiro Meigo*, Hiroshi Takada*, Satoshi Chiba*, Tatsushi Nakamoto**, Kenji Ishibashi**, Naruhiro Matsufuji**, Keisuke Maehata**, Nobuhiro Shigyo**, Yoshihisa Wakuta**, Yukinobu Watanabe† and Masaharu Numajiri††

* Japan Atomic Energy Research Institute, Tokai-mura, Naka-gun, 319-11, Japan
** Department of Nuclear Engineering, Kyushu University, Hakozaki, Fukuoka, 812, Japan
† Energy Conversion Engineering, Kyushu University, Kasuga-koen, Kasuga, 816, Japan
†† National Laboratory for High Energy Physics (KEK), Oho, Tsukuba, 305, Japan

ABSTRACT

Double differential neutron spectra from a thick lead target bombarded with 0.5 and 1.5 GeV protons have been measured with the time-of-flight technique. In order to obtain the neutron spectra without the effect of the flight time fluctuation by neutron scattering in the target, an unfolding technique has also been employed in the low energy region below 3 MeV. The measured data have been compared with the calculated results of NMTC/JAERI-MCNP-4A code system. It has been found that the code system gives about 50 % lower neutron yield than the experimental ones in the energy region between 20 and 80 MeV for both incident energies. The disagreements, however, have been improved well by taking account of the in-medium nucleon-nucleon scattering cross sections in the NMTC/JAERI code.

1. Introduction

With recent progress of the accelerator technology, various utilizations of a high energy and high current proton accelerator are proposed for various purposes such as neutron scattering study and accelerator driven actinide transmutation[1]. For the design of the target and shielding of the accelerator facilities, it is necessary to estimate the reaction rate and the neutron production in a thick medium in the energy region up to several GeV as accurately as possible. Nucleon-Meson Transport Codes such as NMTC/JAERI[2] and LAHET[3] have been widely employed for the neutronics calculation.

It is generally known that the codes can describe the particle productions and the transport in a thick medium. The accuracy of the codes is not completely satisfactory yet. In order to comprehend and improve the accuracy of the code, several studies[4,5] have been performed from both the theoretical and the experimental points of view. A series of measurements of neutron production double differential cross sections were carried out at LANL[6,7,8,9] and KEK[10]. In LANL, the neutron yields in stopping-length targets were also measured with 113 and 256 MeV protons[5,6]. There is only a few data[11,12] on the

Keywords: Neutron spectrum, Time of flight and unfolding technique, NMTC/JAERI, 0.5 and 1.5 GeV

neutron spectra from thick targets bombarded with protons at incident energies higher than 256 MeV.

In this study, the neutron spectra from a thick lead target bombarded with 0.5 and 1.5 GeV protons have been measured at 6 angles between 15° and 150° using the TOF and unfolding techniques. The measured data were compared with calculated results of the NMTC/JAERI-MCNP-4A code system.

2. Experimental Procedure

2.1 *Incident Protons and Target*

The experiment was carried out at the π2 beam line of National Laboratory for High Energy Physics (KEK) in a series of double differential neutron production cross section measurements[10]. The illustration of the experimental arrangement is shown in Fig. 1. The incident proton was supplied as the secondary particle generated by an internal target which was placed in the accelerator ring of the 12 GeV proton synchrotron. The intensity of the incident particles was so weak ($<10^5$ particles/macro pulse) that incident protons were counted one by one with beam scintillators. The size of the incident beam was 2.0 cm in the perpendicular plane and 1.6 cm in the horizontal one in FWHM, respectively. The protons were identified from the pions produced at the internal target by the time-of-flight (TOF) technique with a pair of scintillators (Pilot U) which were located at a separation distance of 20 m. Each Pilot U scintillator was connected with two photomultipliers on opposite sides. The beam damp was a carbon block pile of 0.5 × 0.5 m^2 in the area and 1 m in thickness. The carbon was surrounded by sufficiently thick iron blocks except on the beam-incident surface. The distance from the target to the beam dump was 8.5 m.

The lead target was a rectangular parallelepiped 15 × 15 × 20 cm^3 whose purity was 99.95%. It was thick enough to stop 0.5 GeV protons completely, while it caused the energy loss of 0.26 GeV on average for 1.5 GeV protons.

2.2 *Neutron Detector*

NE213 scintillators having the size of 12.7 cm in diameter and 12.7 cm in thickness were used as neutron detectors. The detectors were placed at angles of 30°, 60°, 90°, 120° and 150° to the beam axis and at a common distance of 1 m from the target. At the angle 15°, the distance was chosen 1.5m so that the higher energy resolution was achieved. In order to reject the events induced by the charged particles (i.e. π, p, d) produced in the lead target, NE102A scintillators of 17 × 17 × 1 cm^3 were used as veto counters. They were placed in front of the NE213 scintillators at a distance of 2 cm.

The pulse height of the neutron detectors was calibrated by standard gamma ray measurements. The gamma ray energies are summarized in Table 1 with the light outputs

Table 1. Light Output at the half height of Compton edge for the source gamma ray

Gamma Ray Source	Energy (MeV)	Light Output (MeVee) [a]
^{137}Cs	0.662	0.493
^{60}Co	1.173, 1.333	1.074 [b]
Am-Be	4.439	4.331

[a] 1 MeVee corresponds to the light output given by 1 MeV electron.

[b] Only one Compton edge is observed, because NE213 has poor resolution to distinguish 2 Compton edges. This light output is calculated with the average energy of 2 gamma rays.

at the half height of Compton edges. The light output was derived from the empirical formula of Dietze[13] and expressed in the unit of electron equivalence. A good linearity between the light output and the measured signal was verified below 4.33 MeVee.

2.3 *Electronic Circuit*

The diagram of the electronic circuit is shown in Fig. 2. When a coincidence of the signals from all beam scintillators took place, a pulse with a time duration of 150 ns was sent to the next coincidence unit. The events arising from incident pions were eliminated with the help of the coincidence pulse of all beam scintillators. The number of incident protons was accumulated by the scaler. A good discrimination for the incident proton against the pion was achieved so that the uncertainty of the counting could be less than 1 %. The TOF spectrum was obtained from the difference of digitized occurrence time between NE213 scintillator and beam scintillators (P01 and P02) pulses.

Anode signals of the photomultipliers connected with NE213 scintillators, were branched out to four pulses. Three pulses and gate signals were supplied to three ADCs that digitized the integrated charge of the pulses during the gate signal independently. The pulse height distribution was obtained from the ADC-3 which collected the total charge of pulse. The other ADC-1,2 digitized the integrated charge of the fast and tail parts of scintillation pulse, in order to reject the events induced by gamma rays employing the two-gate integration method[14]. The conceptual diagram of this method is shown in Fig. 3. All digitized data were taken event by event and stored in the magnetic tape for off-line analyses.

3. Data Analysis

3.1 *TOF Analysis*

Figure 4 shows an example of the TOF spectrum from the target, whose horizontal axis is reversed. A sharp peak due to prompt gamma rays is observed around 3100 channel. The width was typically 1.5 ns in FWHM. After the neutron events were discriminated from the gamma ray ones, the TOF spectrum of the neutrons was obtained as shown in the bottom of Fig. 4. By interposing an iron block of 50 cm in thickness between the target and detector, the room back ground was measured and found to be negligible.

The energy spectrum of the neutron is converted from the net TOF spectrum by the following expression,

$$\frac{d^2n}{dEd\Omega} = \frac{N_n}{N_p\,\varepsilon\,\Delta\Omega\,\Delta E}, \quad E = m_n c^2\left(1/\sqrt{1-L^2/\left(c(t-t_0)+L\right)^2}-1\right) \tag{1}$$

where N_n and N_p are the counts of neutrons and incident protons, respectively, ε the detection efficiency for the neutron, $\Delta\Omega$ the solid angle sustained by the detector to the center of the target, E the neutron energy, t the flight time, m_n the rest mass of the neutron, c the light speed, t_0 the flight time of the prompt gamma ray and L the distance between the centers of target and detector. Here, the distance from the neutron producing point to the detection point is assumed to be L. This assumption was confirmed by a Monte-Carlo calculation which gave the standard deviation of the distance L smaller than 6 %.

The detection efficiencies were calculated for the energy range below 80 MeV with SCINFUL[15] and up to 1.5 GeV with Cecil[16]. The results are shown with the experimental ones in Fig. 5. It is observed that SCINFUL results agree with the experimental data[17,18] much better than Cecil. In the TOF analysis, therefore, the SCINFUL results were used as the detection efficiency below 80 MeV. Above 80 MeV, on the other hand, the

calculated efficiency of Cecil adjusted to connect smoothly with that of SCINFUL at 80 MeV was employed. Two neutron spectra were obtained with two efficiencies using the ^{137}Cs and ^{60}Co biases which were set at the half height of Compton edges for ^{137}Cs and ^{60}Co gamma rays, respectively. The neutron spectra determined with ^{137}Cs bias agreed with those determined with the ^{60}Co bias within the statistical errors. Since the statistical accuracy of the spectra obtained with the ^{137}Cs bias was higher than that of ^{60}Co bias, the results with the ^{137}Cs bias were adopted as the resultant neutron spectra.

3.2 *Unfolding Analysis*

Since the target was thicker than the mean free path for the neutrons with the energy below 200 MeV, most neutrons react with target nuclei more than once in the transport process. The scattered neutron has some delay in the flight time in comparison with the neutron which comes out the target without scattering. The delay makes apparent neutron energy spectrum obtained by the TOF technique softer than the real one. We analyzed the pulse height distribution by the unfolding technique to obtain the neutron spectrum independently. The unfolding analysis employed the code FORIST[19] which used a response matrix calculated with SCINFUL. The neutron spectra in the energy region below 14 MeV were obtained by the unfolding technique, because the pulse height was saturated above 14 MeV.

In Fig. 6, the neutron spectrum at the angle of 30° obtained by the unfolding technique is compared with the one by the TOF technique for 500 MeV proton incidence. In the region below 3 MeV, the difference of the neutron yield was larger than 50 % of that obtained by the TOF technique. This difference is ascribed to the ambiguity of the efficiency around the ^{137}Cs bias used in the TOF technique. Therefore, the neutron spectra derived by the unfolding analysis is more reliable than those obtained by the TOF technique below 3 MeV. The results of unfolding analysis agree with those of TOF quite well between 3 and 14 MeV. This indicates that the time fluctuation by the scattering is negligibly small above 3 MeV. In consequence, the neutron energy spectrum was determined by connecting the result of the TOF technique with that of the unfolding technique at 3 MeV. The error of the unfolding analysis for neutrons below 1.5 MeV was so large that the lowest energy of measured spectra were decided to be 1.6 MeV.

4. Calculation

The calculation was carried out with codes, NMTC/JAERI[2] and MCNP-4A[20]. NMTC/JAERI calculated the nuclear reactions and the particle transport above 20 MeV. MCNP-4A calculated the neutron transport below 15 MeV using a continuous energy cross section library FSXLIB-J3R2[21] processed from the nuclear data file JENDL-3.2[22]. In NMTC/JAERI, the systematics of Pearlstein[23] was implemented to estimate the total, the elastic and non-elastic nucleon-nucleus cross sections in the transport calculation part. The level density parameter derived by Baba[24] was also employed in the statistical decay calculation in NMTC/JAERI.

Additional calculations were also performed by substituting the in-medium nucleon-nucleon cross sections (NNCS) for the free ones in the nuclear reaction calculation part of NMTC/JAERI. In this calculation, were employed the in-medium NNCS parametrized similarly to those by Cugnon[25].

5. Results and Discussion

The present experimental spectra are shown in Figs. 7 and 8. The uncertainty of various quantities is given in Table 2. The uncertainty of the neutron yield was determined from those of the statistical, the neutron detection efficiency and the number of incident protons. The uncertainty of the detection efficiency is estimated at 3.0% for the neutron energy below 20 MeV. With the increase of neutron energy, the uncertainty becomes larger because of the increasing ambiguity the cross section used in the calculation.

The neutron energy resolution is also given in Table 2. It was determined from the uncertainty of the time and the flight path. The time uncertainty is derived from the time resolution of the detector and the fluctuation of the flight time that is spent by an incident proton to move from an incident point to a reaction point. The time resolution of the detector has been determined to be 0.4 ns in the standard deviation by the width of the prompt gamma peak of the thin target measurements[10]. The time fluctuation was approximated to a half value of the transit time of protons in the target which was obtained by Janny[26]. Those are determined 0.6 and 0.4 ns for the 0.5 and 1.5 GeV incident protons, respectively. The uncertainty of the flight path was estimated at 6.0 cm by the Monte-Carlo calculation on condition that the neutrons were produced uniformly in the target and detected uniformly in the detector. Since the correlation between the time fluctuation for incident protons and the flight path is ignored, the real energy resolution will be better than that described here.

Table 2. Uncertainty and energy resolution of neutron spectra expressed in the standard deviation

Neutron Energy (MeV)	Uncertainty (%)				Energy Resolution (%)
	Statistical Error	Detection Efficiency	Number of Incident Proton	Neutron Yield	
3	3 ~ 7	3		4 ~ 7	10 ~ 11
10	5 ~ 10	3		6 ~ 11	10 ~ 11
15	6 ~ 10	3		6 ~ 11	12 ~ 13
20	6 ~ 10	10	1	6 ~ 11	12 ~ 14
50	8 ~ 30	10		13 ~ 32	13 ~ 17
100	7 ~ 46	15		17 ~ 46	16 ~ 22
200	11 ~ 20*	15		19 ~ 25*	20 ~ 32

* For the angle smaller than 90°

Figure 9 shows a comparison between the present data for 1.5 GeV proton bombardment and the measured one at JINR[11]. In the experiment at JINR, a lead target having the size of 20 cm in diameter and 20 cm in length was bombarded with 2.55 GeV protons. It is found that the present neutron energy spectrum is quite similar to those obtained at JINR, although the incident proton energies are different.

The calculated results of the NMTC/JAERI-MCNP-4A code system, which are smeared with the energy resolution, are also shown in Figs. 7 and 8. It is observed that the results calculated with the free NNCS are in good agreement with the experimental ones in the lower energy region below 20 MeV at all angles for both incident energies. The calculated results, however, are about 50 % or more lower than the experimental data between 20 and 80 MeV at all angles. On the other hand, the results calculated with the in-medium NNCS show much better agreement with the experimental ones in this energy region. This improvement is ascribed to the fact that the increase of the high energy nucleon emission

diminishes the excitation energy of a residual nucleus so that the neutron emission from the evaporation process is suppressed. The calculation with the in-medium NNCS successfully reproduces the overall measured neutron spectra in the angular region smaller than 60° for both incident energies although the codes give slightly lower neutron yields below 10 MeV. The underestimation for the backward neutron emission, however, still remains.

In order to investigate the cause of the discrepancy between the calculations and the experiments, the double differential neutron production cross sections were also calculated with the in-medium NNCS for the incident energies of 0.8 and 1.5 GeV, respectively. The results are compared with the experiments[9,10] in Figs. 10 and 11. It is found that the agreement between the calculated and the experimental results for the thick target is as in the same level for that in the thin target. This indicates that the nuclear reaction calculation part should be improved in NMTC/JAERI. Some studies[5,27] showed that the inclusion of the preequilibrium process or the refraction and reflection process improved the backward neutron emission significantly. By the inclusion of those processes, the disagreement of the thick target will be more improved.

6. Conclusion

The neutron spectra from a thick lead target bombarded with 0.5 and 1.5 GeV protons were measured at 6 angles between 15° and 150°. We have obtained the precise neutron spectra in the energy region above 1.6 MeV using the TOF and unfolding techniques with the neutron yield uncertainty of 7 % at 3 MeV and 25 % at 200 MeV. The calculation was also carried out with the NMTC/JAERI-MCNP-4A code system. It was found that results showed fairly good agreement with the experiments, but gave about 50 % lower neutron yield in the energy region between 20 and 80 MeV. The calculation with the in-medium NNCS achieved good agreement with the experiments. The calculation, however, could not reproduce well the backward neutron emission. It is of interest to make systematic experiments with other targets for further investigation of the accuracy of NMTC/JAERI including the in-medium NNCS.

References

[1] For example, T. Takizuka, et al., *Conceptual Design Study of an Accelerator-based Actinide Transmutation Plant with Sodium-cooled Solid Target/Core,* Proc. of OECD/NEA Mtg., Argonne (1993) 398

[2] Y. Nakahara and T. Tsutsui, *A Code System for High Energy Nuclear Reactions and Nucleon-Meson Transport Code, JAERI-M 82-198 (1982),* [in Japanese]

[3] R. E. Prael and H. Lichtenstein, *Users Guide to LCS: The LAHET Code System,* LA-UR 89-3014 (1989)

[4] *Intermediate Energy Nuclear Data: Models and Code,* Proc. of OECD/NEA Mtg., Paris (1994)

[5] N. Yoshizawa, K. Ishibashi and H. Takada, *J. Nucl. Sci. Technol.* **32** (1995) 601

[6] M. M. Meier, et al., *Nucl. Sci. and Eng.* **102** (1989) 309

[7] M. M. Meier, et al., *ibid.* **104** (1990) 339

[8] S. Stamer, et al., *Phys. Rev.* **C47** (1993) 1647

[9] M. M. Meier, et al., *Rad. Eff.* **96** (1986) 73

[10] K. Ishibashi, et al., *Measurement of Neutron-Production Double-Differential Cross Sections for Incident Protons of 0.8, 1.5 and 3 GeV,* Proc. Int. Conf Nucl. Data for Sci. and Technol., Gatlinburg (1994)

[11] A. D. Kirillov, et al., JINR-P-13-90-193 (1990)
[12] S. Cierjacks, et al., *Phys. Rev.* **C193** (1987) 1976
[13] G. Dietze and H. Klein, *Nucl. Instrum. Meth.* **193** (1982) 529
[14] Z. W. Bell, *ibid.* **188** (1981) 105
[15] J. K. Dickens, *SCINFUL: A Monte Carlo Based Computer Program to Determine a Scintillator Full Energy Response to Neutron Detection for En Between 0.1 and 80 MeV,* ORNL-6436 (1988)
[16] V.V. Verbinski, et al., *The Response of Some Organic Scintillators to Fast Neutrons,* ORNL-P-993 (1965)
[17] S. Meigo, et al., private communication
[18] R. A. Cecil, et al., *Nucl. Instrum. Meth.*, **161** (1979) 439
[19] R. H. Johnson and B. W. Wehring, *The FORIST UNFOLDING CODE,* ORNL/RSIC-40 (1976) 33
[20] J. F. Briesmeister (Ed.), *MCNP A General Monte Carlo N-Particle Transport Code Version 4A*, LA-12625 (1993)
[21] K. Kosako, et al., *A Continuous Energy Cross Section Library for MCNP Based on JENDL-3.2,* JAERI-Data/Code 94-020 (1994)
[22] K. Shibata, et al., *Japanese Evaluated Nuclear Data Library, Version-3 -JENDL-3-,* JAERI-1319 (1990)
[23] S. Pearlstein, *Astrophys. J.* **346** (1989) 1049
[24] H. Baba, *Nucl. Phys.* **A159** (1970) 625
[25] J. Cugnon, T. Mizutani and J. Vandermeulen, *ibid.* **A352** (1981) 505
[26] J. F. Janny, *Atom. Data and Nucl. Data Tables* **27** (1982) 147
[27] H. Takada, submitted to *J. Nucl. Sci. Technol.*

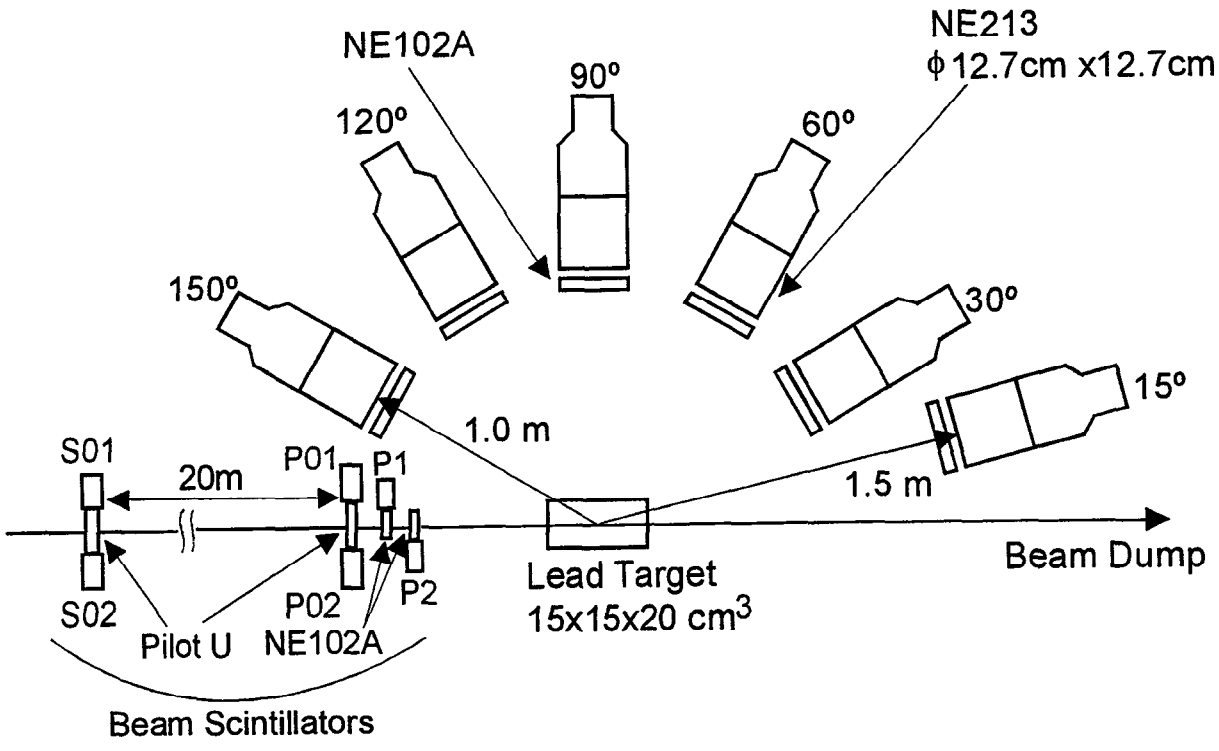

Fig. 1 Illustration of the experimental arrangement

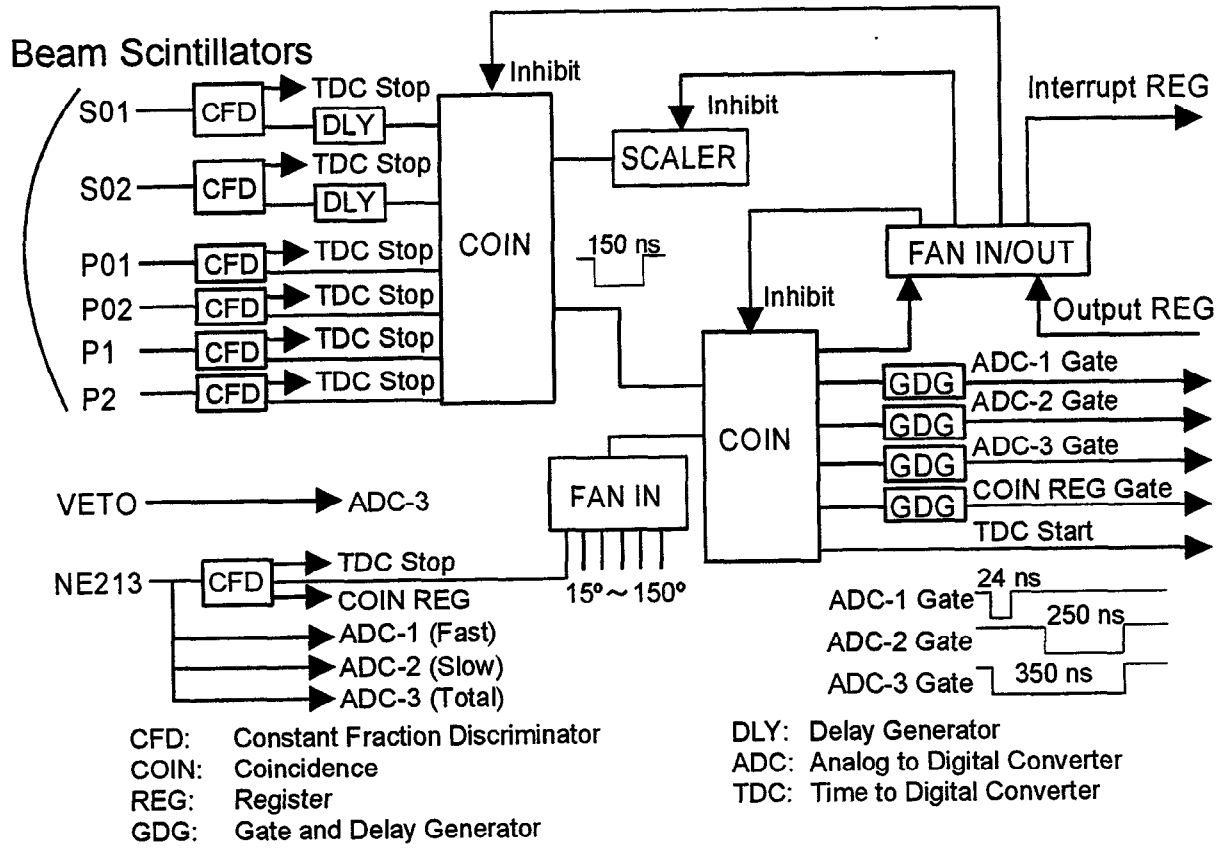

Fig. 2 Diagram of the electronic circuit used in the present experiment

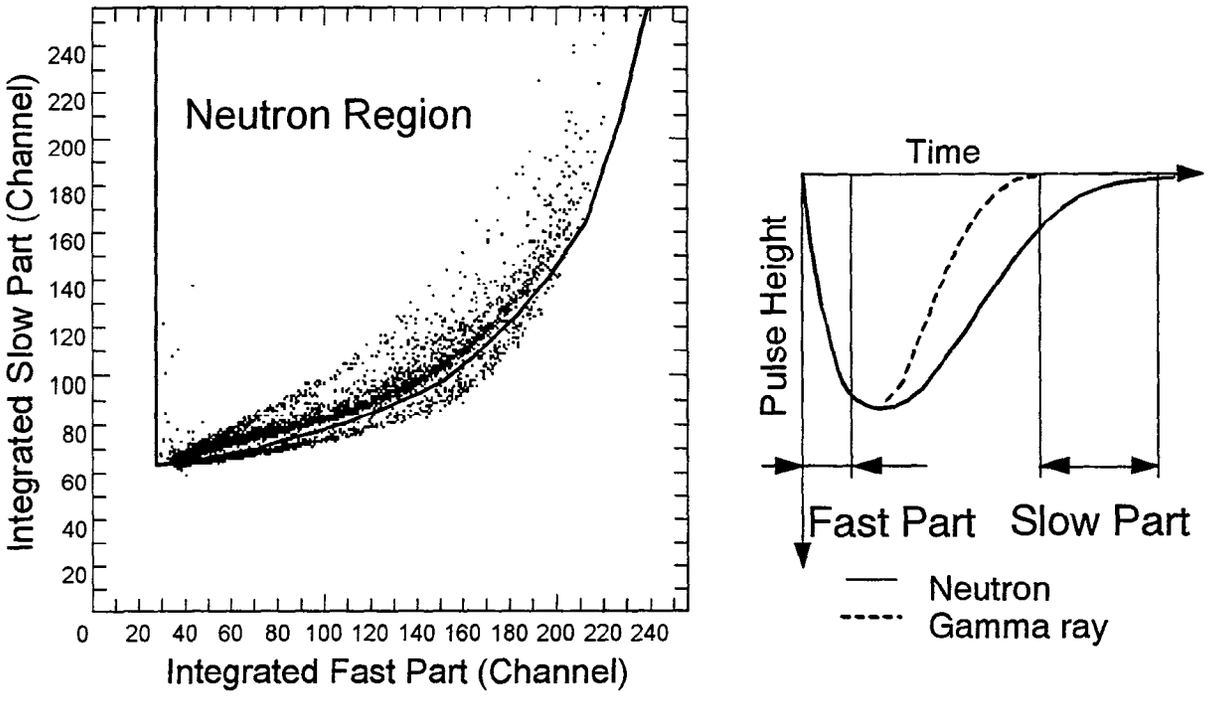

Fig. 3 Conceptual diagram of the two-gate integration method of neutron-gamma discrimination

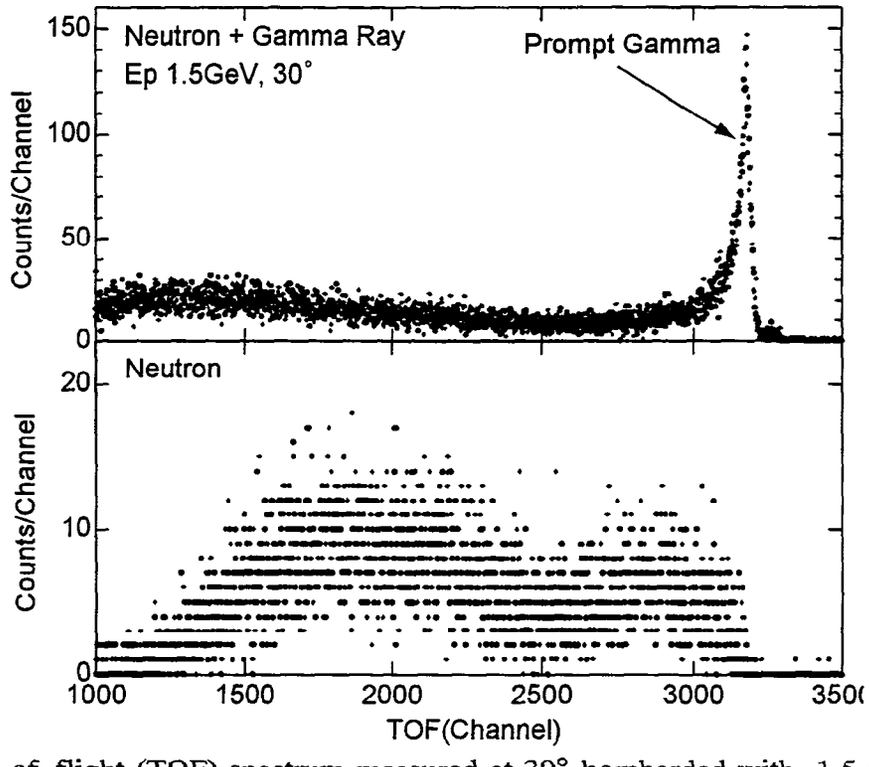

Fig. 4 Time-of-flight (TOF) spectrum measured at 30° bombarded with 1.5 GeV protons (top; for the neutron and the gamma ray, bottom; only for the neutron). Width of the TOF bin is 28 ps/channel.

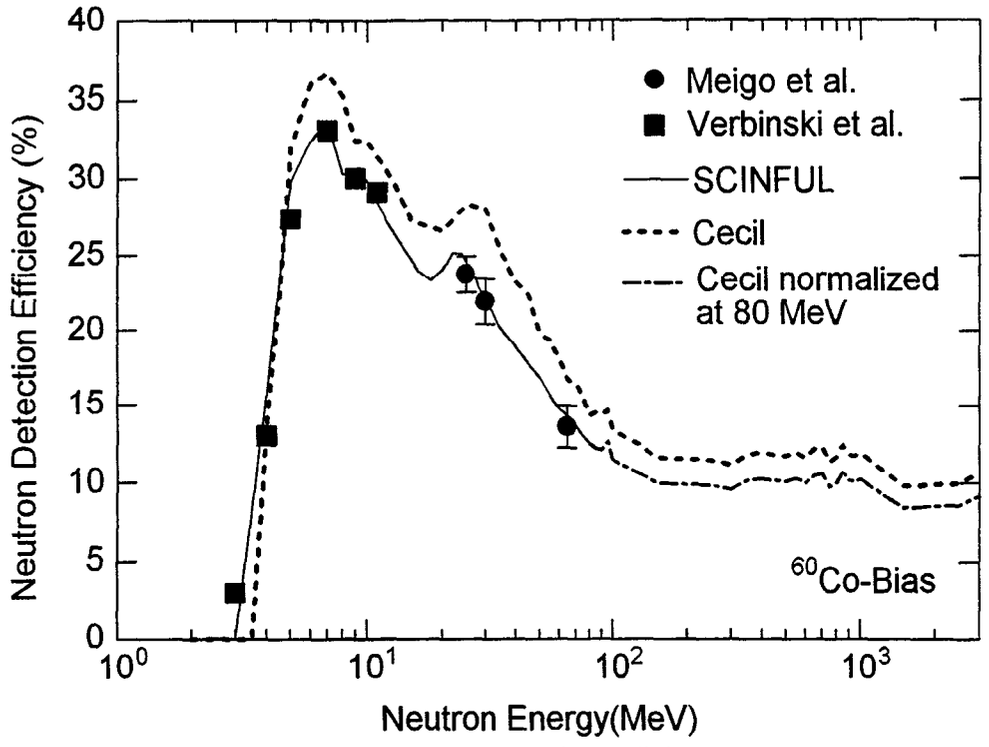

Fig. 5 Calculated and experimental neutron detection efficiency of the NE213 scintillator having the size of 12.7 cm in diameter and 12.7 cm in thickness

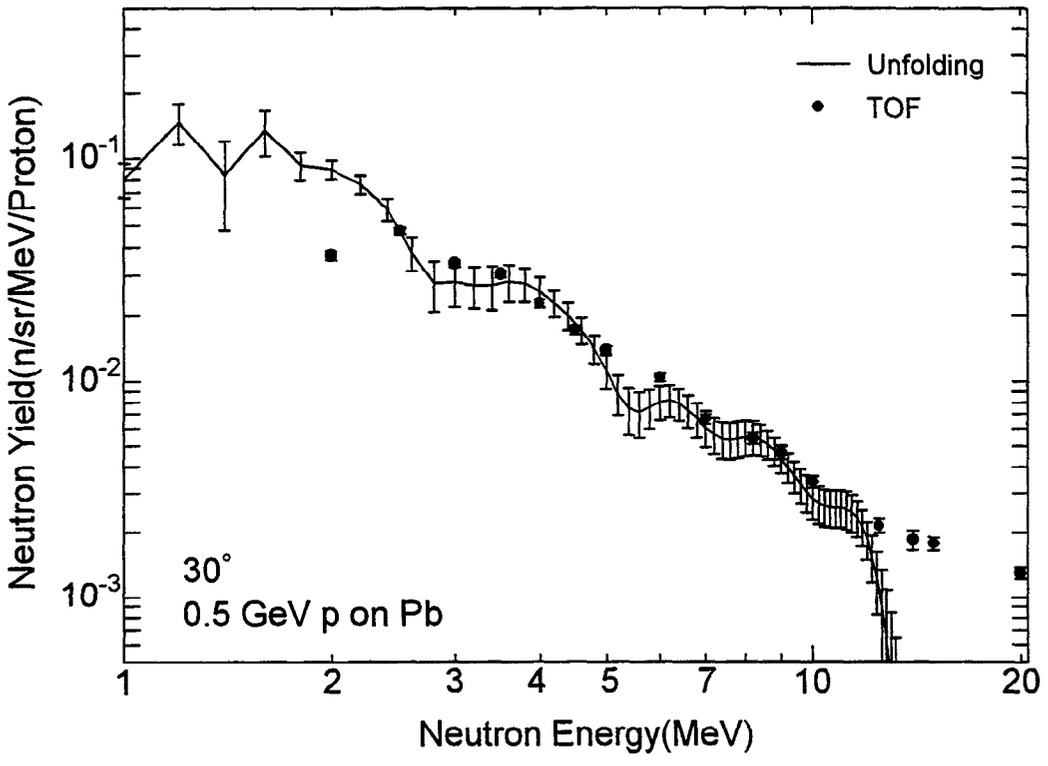

Fig. 6 Comparison of the neutron spectra at 30° obtained by TOF and unfolding methods for 0.5 GeV proton incident on thick lead target

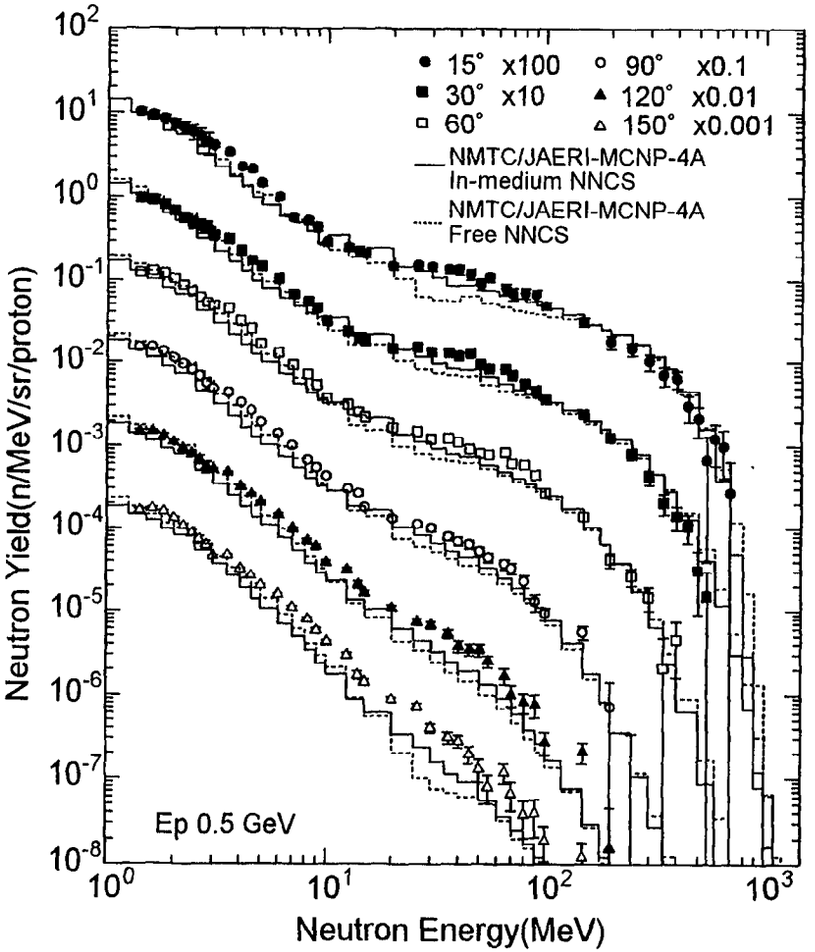

Fig. 7 Experimental and calculated neutron spectra in a lead target bombarded with 0.5 GeV protons. The marks are the experimental data. The dashed and the solid lines indicate the calculated results of the code system with free NNCS and those with in-medium NNCS, respectively.

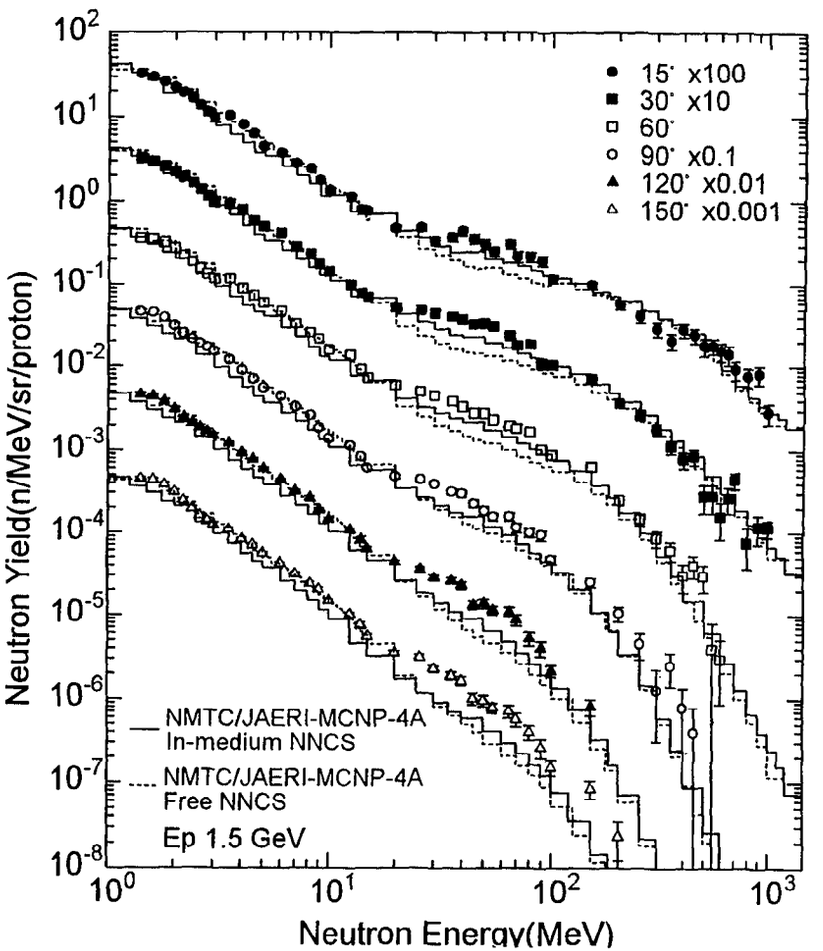

Fig. 8 Same as for Fig. 7, except for proton energy, 1.5 GeV

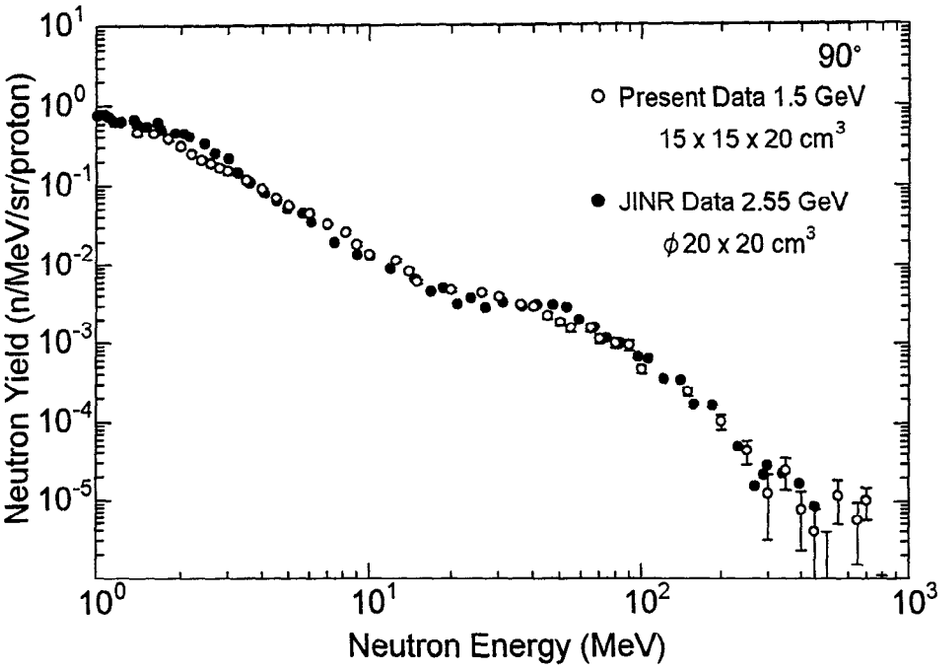

Fig. 9 Comparison of experimental neutron spectrum between the present and the measured one at JINR

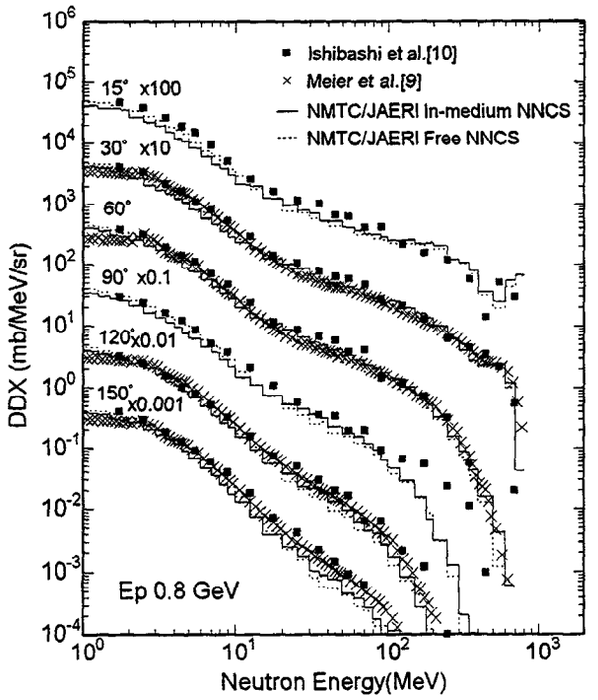

Fig. 10 Double differential neutron production cross sections for 0.8 GeV protons. The solid marks indicate the experimental data[9,10]. The solid and the dash lines show the results of NMTC/JAERI with free NNCS and those with in-medium NNCS, respectively.

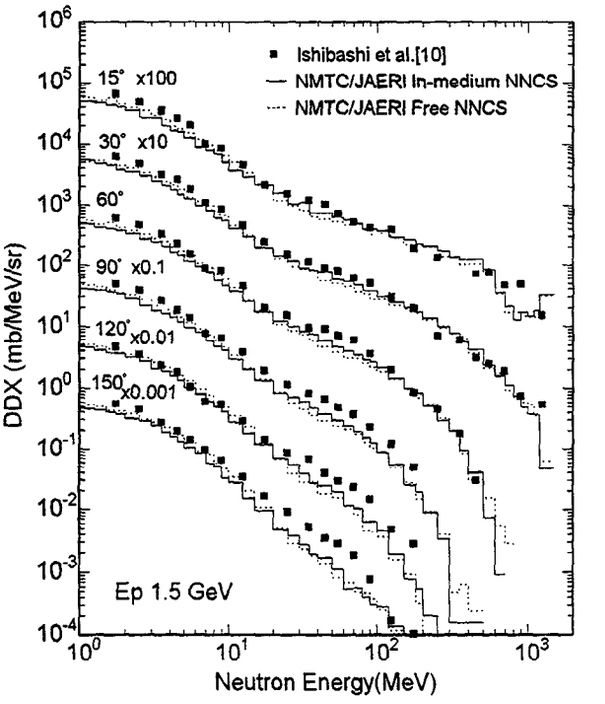

Fig. 11 Same as for Fig.10, except for proton energy 1.5 GeV